A&A manuscript no.
(will be inserted by hand later)

Your thesaurus codes are:
1 (09.04.1; 09.08.1; 09.13.2; 10.03.1; 13.09.4)

ASTRONOMY
AND
ASTROPHYSICS
31.10.1996

Letter to the Editor: first results from ISO

ISOCAM CVF observations of the Quintuplet and Object#17 clusters near the Galactic Center *

T. Nagata[1], **K. Kawara**[2,3], **T. Onaka**[4], **Y. Kitamura**[2], **and H. Okuda**[2]

[1] Department of Physics, Nagoya University, Nagoya 464-01, Japan (nagata@zlab.phys.nagoya-u.ac.jp)
[2] Institute of Space and Astronautical Science, Yoshinodai, Sagamihara 229, Japan
[3] ISO Science Operations Centre, Astrophysics Division of ESA, Villafranca, 28080 Madrid, Spain
[4] Department of Astronomy, University of Tokyo, Tokyo 113, Japan

Received July 15, 1996; accepted August –, 1996

Abstract. Two fields near the Galactic Center, containing the Quintuplet and Object #17 star-clusters, have been imaged with the ISOCAM circular variable filters (CVFs) in the wavelength range of 2.47 – 3.08μm and 3.99 – 9.09μm. Emission of [Ar II] 6.99μm is detected in the "pistol-shaped" H II region (G0.15-0.05) to the south of the Quintuplet cluster. Absorption probably due to O-H stretching vibration (2.8μm) is evident in the Quintuplet spectra. In addition, Quintuplet members and the central part of Object #17 have CO_2(4.3μm) and CO (4.7μm) absorption. Abundant CO_2 might be present in these lines of sight.

Key words: dust, extinction – H II regions – ISM: molecules – Galaxy: center – Infrared: interstellar: lines

1. Introduction

When studying interstellar extinction in the infrared, to find suitable background continuum sources is a difficult issue. The line of sight to the central parsec of the Galaxy is usually regarded as representing diffuse interstellar medium. The absorption features in the spectrum of Sgr A (Willner et al. 1979) are thus thought to be characteristic of diffuse clouds. However, this region is very complicated. For example, many stars are late-type giants, but there are also H II regions and He emission line stars (Krabbe et al. 1991). In addition, a molecular cloud component of extinction seems to exist along the line of sight to the Galactic Center because some infrared sources show deep H_2O ice absorption (IRS 19: Willner & Pipher 1982) and solid CO absorption (IRS 12: McFadzean et al. 1989).

We now know two other star clusters near the Galactic Center which may be used as background continua; one is the Quintuplet cluster at ($l = 0.^\circ16, b = -0.^\circ06$), and the other is the Object #17 cluster at ($l = 0.^\circ12, b = 0.^\circ02$). The Quintuplet, first found in a polarimetric survey by Kobayashi et al. (1983), includes five very bright stars whose color temperatures are in the range of 600–900K (Okuda et al. 1990; Nagata et al. 1990). Object #17 is a cluster of emission line stars (Nagata et al. 1993, 1995; Cotera et al. 1996), which might be similar to the central parsec cluster. These star clusters are also intriguing in themselves.

In this Letter, we report the spectroscopic observations of these two objects with the ISOCAM (Kessler et al. 1996; Cesarsky et al. 1996).

2. Observation and Reduction

The Quintuplet was observed on February 24 and Object #17 on February 23, 1996, with the ISOCAM circular variable filters (CVFs). ISOCAM consists of two optical channels: short wavelength (SW) and long wavelength (LW). In the SW observations, the CVF ($\lambda/\Delta\lambda = 41$) was rotated every 3 steps (0.075μm) from 2.474μm to 3.079μm and from 3.987μm to 5.122μm. The field of view was $45'' \times 45''$ ($1.''5$/pixel). In the LW observations, the CVF ($\lambda/\Delta\lambda \sim 40$) was rotated every 3 steps from 5.079μm to 9.09μm. The field of view was $87'' \times 87''$ ($3''$/pixel). The SW and LW CVF scans were made in the direction of increasing wavelengths, and six exposures were taken at

Send offprint requests to: T. Nagata

* Based on observations with ISO, an ESA project with instruments funded by ESA Member States (especially the PI countries: France Germany, the Netherlands and the United Kingdom) and with the participation of ISAS and NASA.

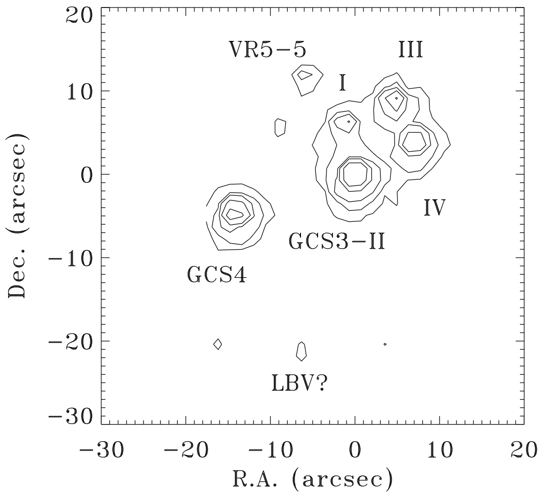

Fig. 1. The Quintuplet cluster at 5.05μm. Contour levels are 0.2, 0.5, 1, 2, and 4 Jy/1$''$.5 pixel.

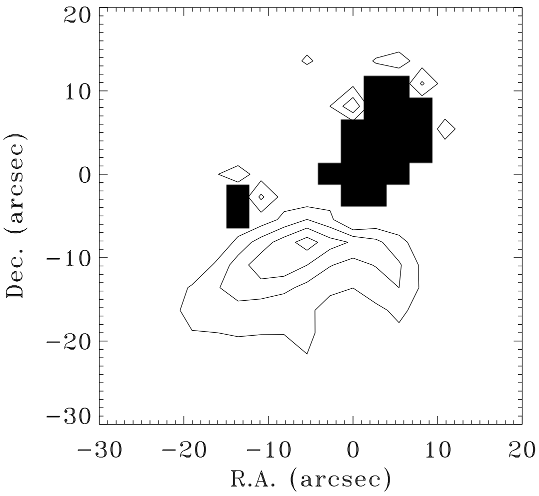

Fig. 2. The Quintuplet field at 7.02μm. Adjacent continua at 6.86 and 7.19μm were subtracted. Black regions are the pixels saturated in the LW observation. Contour levels are 0.1, 0.2, 0.3, and 0.4 Jy/3$''$ pixel.

each wavelength. The exposure time was 6 sec for SW and 5 sec for LW.

We followed standard reduction procedures described in the ISO Data Users Manual by Siebenmorgen et al. (1995), using the ISOCAM libraries of dark current and flat fields. IDL (Interactive Data Language) was used, and deglitching was made with a median filter with width 3. The memory effect due to the long time constant of the detector arrays was examined by comparing the first-exposure spectra with the last-exposure spectra, where the first and last-exposure spectra comprise only data taken in the first and last exposures, respectively, at each CVF wavelength. No systematic differences were found in the SW spectra, but there were systematic differences in the LW spectra. The shifts were largest in the region where the flux level changes rapidly (e. g., from 8.3 to 9.1μm), and the maximum shift is 10% of the flux level. The reader should be reminded that no corrections for the memory effect were made, so that the LW spectra must have been smoothed by this effect to some degree. Also note that the spectra presented here are simple medians of data in every exposure.

At the beginning of the LW CVF scan, pixels exposed to the bright Quintuplet sources were saturated. The data of these sources were missed, but as a trade-off, faint diffuse sources were measured with good signal-to-noise ratios.

The absolute fluxes have been calibrated against the ground-based observations in Table 1 (Okuda et al. 1990: since their table has typographical errors, the correct magnitudes are shown below.) for the Quintuplet region, and the observations with a 6$''$ aperture (Nagata et al. 1993) for Object #17.

Table 1. Magnitudes of Quintuplet in 1986

source	K	L	M	N	Q	[7.8]	[8.7]
GCS 4		3.4	1.9	0.9	0.4	0.7	1.0
GCS 3-I	7.8	4.6	3.2	2.4	1.2	1.9	2.5
GCS 3-II	6.3	2.7	1.2	0.1	-0.6	-0.4	0.2
GCS 3-III	9.4	4.8	2.7	0.4	-1.4	0.6	0.9
GCS 3-IV	7.8	4.3	2.6	0.7	-0.8	0.6	1.0

There is a considerable scattered-light component. It consists of real diffuse flux from background stars and some instrumental flux like ghosts. We can see an out-of-focus image of the primary mirror over the entire field at a very low flux level in the LW channel, but it is impossible to distinguish it from the real diffuse background. Therefore, we chose "sky" regions in the frame and examined their spectra. In Quintuplet, we chose a region to the west of GCS 3-IV as "sky". In Object #17, we chose a region of low stellar density to the northwest of the center in the figures of Nagata et al. (1995) and Figer (1995). As long as the sky levels are insignificant, we can securely regard the object signals as real.

3. Results

The Quintuplet cluster field is shown in Figs. 1 and 2. Fig. 1 is a continuum image at 5.05μm; the five brightest members and the sixth source (VR5-5 in Moneti et al. 1994) are clearly seen. In Fig. 3, the spectra of 6$''$ × 6$''$ around the peaks of these sources after subtracting the "sky" flux

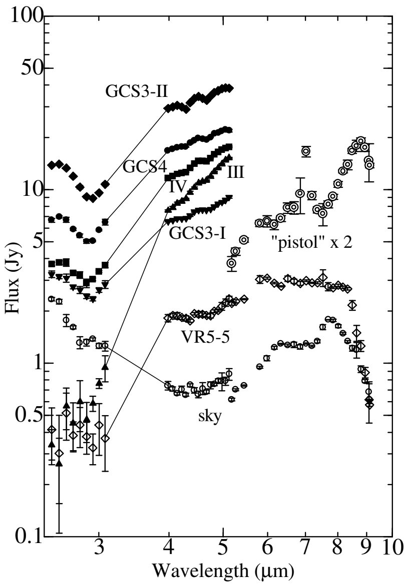

Fig. 3. CVF spectra of Quintuplet sources. The fluxes in $6'' \times 6''$ regions have been summed. For the "pistol" region, $21'' \times 9''$ flux is plotted (In the short wavelength region little signal was detected) after multiplication by 2 for clarity. These source fluxes are after subtraction of the sky flux, which is the summed and normalized signal of the region to the west of GCS 3-IV. The plotted sky flux is converted to that in a $6'' \times 6''$ region.

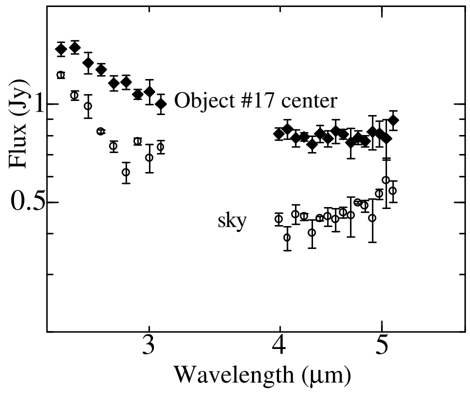

Fig. 4. CVF spectra of the central $6''\times 6''$ region of Object #17 after subtraction of the sky flux. The sky flux is the summed signal of the region to the northwest (normalized to $6'' \times 6''$).

are shown. Standard deviations of median-filtered data are shown as error bars to aid estimating fluctuations, but these are generally smaller than systematic errors such as the selection of the "sky" area. Similarly, the spectrum of central $6'' \times 6''$ region of the Object #17 cluster is shown in Fig. 4. This region includes emission line stars 7, 8, 10, and probably 11 in Nagata et al. (1995).

Fig. 2 is a 7.02μm Quintuplet image after subtracting adjacent wavelengths. The "pistol-shaped" H II region (G0.15-0.05) to the south of the five stars is bright at this wavelength. We identify this to be the fine-structure [Ar II] line at 6.99μm. The line intensity from the $21''(\alpha) \times 9''(\delta)$ region around the peak is 4.8 (-14) W m^{-2}. The spectrum of this region is shown in Fig. 3.

This line is most prominent in the 4 to 8μm spectrum of Sgr A (Willner et al. 1979; Lester et al. 1981). Willner et al. (1979) use the radio continuum emission of 26 Jy at 5 GHz in a $0'.6 \times 1'$ beam (Ekers et al. 1975), and predict the intensity of [Ar II] line from Sgr A. Their measured [Ar II] flux 6.4 (-13) W m^{-2} is twice the predicted flux, and they suggest overabundance of argon in the Galactic Center. In the "pistol" region, Yusef-Zadeh, Morris, & Gorkom (1989) measured radio recombination lines and made a simple model of optically thin ionized plasma. Their model uses a 5 GHz continuum flux of 0.6 Jy, and the resultant number of ionizing photons is 3.9 (48) s^{-1}. Moneti et al. (1994) found He I emission in the "ridge" source on the west of the GCS 3 cluster, and Br γ and He I emission in the "pistol" region. In addition, Figer et al. (1995) have recently observed an emission-line star near the "pistol" region (Star 3, which is #25 in Nagata et al. 1993 and the "serendipitous" source in Moneti et al. 1994; this star appears as the lowest contour in Fig. 1), and concluded that this star is similar to luminous blue variables (LBVs). They suggest that it can produce 3.4 (48) s^{-1} ionizing photons. Thus, the radio contimuum and the [Ar II] line fluxes from the "pistol" are probably consistent with the picture of optically thin H II region powered by the LBV candidate and/or the "ridge" source.

In Fig. 3, we find a broad absorption feature at 2.8μm and dips at 4.3μm and at 4.7μm in all the objects detected with sufficient signal-to-noise ratios. Similar dips seem to be present in Fig. 4 at 4.3μm and 4.7μm.

The 2.8μm absorption is probably due to O-H stretching vibration. This absorption feature is marginally present in the ground-based observations (Okuda et al. 1990), and it is now clearly shown thanks to the presence of the 2.5–2.8μm part of spectra. The O-H bending mode at 6.1μm, whose absorption intensity in H_2O is more than one magnitude weaker (Tielens et al. 1996), is not present in the spectra. The 2.8μm absorption seems to be distributed inhomogeneously in the direction of the Galactic Center because it is not seen in Object #17. This is reminiscent of the 3μm absorption in the central parsec; Galactic Center IRS 19 has a deep feature, but those for IRS 3 and IRS 7 are much shallower (McFadzean et al. 1989). We are not certain what material causes this 2.8μm absorption, but possible candidates are: 1) hydrated silicate in diffuse interstellar medium (Knacke et al. 1982, see also Wada et al. 1991), 2) water ice in molecular clouds, and 3) water vapor in the stellar atmosphere. Water ice is not a very likely candidate because the maximum absorption of water ice is usually at 3.0 – 3.1μm (e. g., Smith et al. 1989), and that for IRS 19 is at only slightly shortward of 3.0μm (McFadzean et al. 1989). Water vapor is also unlikely because the Quintuplet spectra are smooth in the K band without a trace of the CO overtone bands near 2.3μm and the H_2O band near 1.9μm (Okuda et al. 1990).

The 4.7μm absorption is caused by CO. In Quintuplet, Okuda et al. (1990) detected the P and R branches of the gaseous CO v=0-1 band. They have derived the column density of CO to be 1 (18) cm^{-2}. Since Okuda et al. did not detect solid CO, the line of sight to the Quintuplet cluster is free of densest parts of molecular clouds where solid CO exists. This is consistent with the absence of (deep) water ice absorption.

The 4.3μm absorption is due to strong CO_2 resonance. The absorption τ at 4.3μm in the CVF measurement of $\Delta\nu = 57$cm^{-1} is $\sim$ 0.1 for GCS 3-II and Object #17, and $\sim$ 0.04 for other GCS 3 sources and GCS 4. We are uncertain whether the difference in τ between GCS 3-II and other Quintuplet members is significant. The absorption intensity of gaseous CO_2 (1 (-16) cm molecule^{-1}: Gribov & Smirnov 1962) is not very different from those of solid CO_2 in various ices (7 (-17) – 2 (-16) cm molecule^{-1}: Sandford et al. 1988; Sandford & Allamandola 1990). Although CO_2 is unlikely to have appreciable abundance from gas chemistry (Herbst & Leung 1986), CO_2 can form on the grains and its high production rate influences the gas phase (d'Hendecourt et al. 1986). Since CO is in the gas phase toward the Quintuplet, we tentatively adopt the gas absorption intensity of CO_2 and calculate its column density. If we use τ of 0.05, the column density of CO_2 is 3 (16) cm^{-2}. This is 1/30 of the CO column density (Okuda et al. 1990), and it can be the second abundant molecule. It is necessary to locate this CO_2 and establish whether it is in the gas or solid phase.

Acknowledgements. We wish to thank the ISO team for realizing this wonderful satelite project.

References

Cesarsky, C. J., et al. 1996, A&A, this volume
Cotera, A. S., Erickson, E. F., Colgan, W. J., Simpson, J. P., Allen, D. A., & Burton, M. G. 1996, ApJ, 461, 750
d'Hendecourt, L. B., Allamandola, L. J., Grim, R. J. A., & Greenberg, J. M. 1986, A&A, 158, 119
Ekers, R. D., Goss, W. M., Schwarz, U., J., Downes, D., & Rogstad, D. H. 1975, A&A, 43, 159
Figer, D. F. 1995, Ph. D. Thesis, University of California at Los Angeles
Figer, D. F., McLean, I. S., & Morris, M. 1995, ApJ, 447, L29
Gribov, L. A., & Smirnov, V. N. 1962, Sov. Phys. Usp., 4, 919
Herbst, E., & Leung, C M. 1986, MNRAS, 222, 689
Kessler, M. F., et al. 1996, A&A, this volume
Knacke, R. F., McCorkle, S., Puetter, R. C., Erickson, E. F., & Kratschmer, W. 1982, ApJ, 260, 141
Kobayashi, Y., Okuda, H., Sato, S., Jugaku, J., & Dyck, H. M. 1983, PASJ, 35, 101
Krabbe, A., Genzel, R., Drapatz, S., & Rotaciuc, V. 1991, ApJ, 382, L19
Lester, D. F., Bregman, J. D., Witteborn, F. C., Rank, D. M., & Dinerstein, H. L. 1981, ApJ, 248, 524
McFadzean, A. D., Whittet, D. C. B., Longmore, A. J., Bode, M. F., & Adamson, A. J. 1989, MNRAS, 241, 873
Moneti, A., Glass, I. S., & Moorwood, A. F. M. 1994, MNRAS, 268, 194
Nagata, T., Woodward, C. E., Shure, M., Pipher, J. L., & Okuda, H. 1990, ApJ, 351, 83
Nagata, T., Hyland, A. R., Straw, S. M., Sato, S., & Kawara, K. 1993, ApJ, 406, 501
Nagata, T., Woodward, C. E., Shure, & Kobayashi. N. 1995, AJ, 109, 1676
Okuda, H., Shibai, H., Nakagawa, T., Matsuhara, H., Kobayashi, Y., Kaifu, N., Nagata, T., Gatley, I., & Geballe, T. R. 1990, ApJ, 351, 89
Sandford, S. A., Allamandola, L. J., Tielens, A. G. G. M., & Valero, G. J. 1988, ApJ, 329, 498
Sandford, S. A. & Allamandola, L. J. 1990, ApJ, 355, 357
Smith, R. G., Sellgren, K., & Tokunaga, A. T. 1989, ApJ, 344, 413
Tielens, A. G. G. M., Wooden, D. H., Allamandola, L. J., Bregman, J., & Witteborn, F. C. 1996, ApJ, 461, 210
Wada, S., Sakata, A., & Tokunaga, A. T. 1991, ApJ, 375, L17
Willner, S. P., Russel, R. W., Puetter, R. C., Soifer, B. T., & Harvey, P. M. 1979, ApJ, 229, L65
Willner, S. P., & Pipher, J. L. 1982, in: The Galactic center, AIP Conf. Proc. No.83, eds. G. R. Reigler, R. D. Blandford, AIP, New York, p. 77
Yusef-Zadeh, Morris, & Gorkom 1989, in: The Center of the Galaxy, IAU Symp. 136, ed. M. Morris, Kluwer, Dordrecht, p. 275

This article was processed by the author using Springer-Verlag LaTeX A&A style file *L-AA* version 3.